**The EMBO Journal** Vol. 22 No. 15 pp. 3844–3854, 2003

# Impaired insulin secretion and glucose tolerance in β cell-selective $Ca_V1.2$ $Ca^{2+}$ channel null mice

**Verena Schulla[1], Erik Renström[2,3], Robert Feil[1], Susanne Feil[1], Isobel Franklin[4], Asllan Gjinovci[4], Xing-Jun Jing[2], Dirk Laux[1], Ingmar Lundquist[2], Mark A.Magnuson[5], Stefanie Obermüller[2], Charlotta S.Olofsson[2], Albert Salehi[2], Anna Wendt[2], Norbert Klugbauer[1], Claes B.Wollheim[4], Patrik Rorsman[2] and Franz Hofmann[1]**

[1]Institut für Pharmakologie und Toxikologie, TU München, Biedersteiner Strasse 29, D-80802 München, Germany, [2]Department of Physiological Sciences, Lund University, BMC F11, SE-221 84 Lund, Sweden, [4]Division of Clinical Biochemistry, University Medical Center, 1 rue Michel-Servet, CH-1211 Geneva 4, Switzerland and [5]Department of Molecular Physiology and Biophysics, Vanderbilt University School of Medicine, Nashville, TN 37232, USA

[3]Corresponding author
e-mail: erik.renstrom@mphy.lu.se

**Insulin is secreted from pancreatic β cells in response to an elevation of cytoplasmic $Ca^{2+}$ resulting from enhanced $Ca^{2+}$ influx through voltage-gated $Ca^{2+}$ channels. Mouse β cells express several types of $Ca^{2+}$ channel (L-, R- and possibly P/Q-type). β cell-selective ablation of the gene encoding the L-type $Ca^{2+}$ channel subtype $Ca_v1.2$ ($\beta Ca_v1.2^{-/-}$ mouse) decreased the whole-cell $Ca^{2+}$ current by only ~45%, but almost abolished first-phase insulin secretion and resulted in systemic glucose intolerance. These effects did not correlate with any major effects on intracellular $Ca^{2+}$ handling and glucose-induced electrical activity. However, high-resolution capacitance measurements of exocytosis in single β cells revealed that the loss of first-phase insulin secretion in the $\beta Ca_v1.2^{-/-}$ mouse was associated with the disappearance of a rapid component of exocytosis reflecting fusion of secretory granules physically attached to the $Ca_v1.2$ channel. Thus, the conduit of $Ca^{2+}$ entry determines the ability of the cation to elicit secretion.**

*Keywords*: $Ca^{2+}$ channels/diabetes/exocytosis/insulin secretion/pancreatic β cells

## Introduction

Insulin secretion occurs upon elevation of the blood glucose concentration, when the pancreatic β cell depolarizes and regenerative electrical activity consisting of $Ca^{2+}$-dependent action potentials is initiated (Henquin and Meissner, 1984; Ashcroft and Rorsman, 1989). The resultant elevation of the cytoplasmic $Ca^{2+}$ concentration culminates in exocytosis of insulin-containing secretory granules (Barg *et al*., 2001; (Maecheler and Wollheim, 2001). Mouse pancreatic β cells contain dihydropyridine-sensitive L-type $Ca^{2+}$ channels and glucose-induced insulin secretion is almost abolished by pharmacological inhibitors of L-type $Ca^{2+}$ channels such as nifedipine. The molecular identity of the pancreatic β cell L-type $Ca^{2+}$ channel has not been established and it has variably been reported to be $Ca_v1.2$ ($\alpha1_C$) (Barg *et al*., 2001) or $Ca_v1.3$ ($\alpha1_D$) (Yang *et al*., 1999). A significant fraction (~50%) of the whole-cell $Ca^{2+}$ current is resistant to nifedipine (Gilon *et al*., 1997), indicating the presence of additional $Ca^{2+}$ channel subtypes in the β cell. The physiological roles of the non-L-type $Ca^{2+}$ channels are unknown.

Glucose-induced insulin secretion follows a biphasic time-course. A transient first phase lasting 5–10 min is followed by a sustained second phase (Curry *et al*., 1968). The cellular background to the two phases of release remains unknown but it has been suggested to reflect the sequential release of distinct pools of granules, which vary with regard to release competence (Barg *et al*., 2002; Bratanova-Tochkova *et al*., 2002). In support of this idea, high-resolution capacitance measurements have documented two components of exocytosis (Renström *et al*., 1996; Eliasson *et al*., 1997). The rapid component is believed to reflect the release of a limited pool of readily releasable granules in close proximity to the L-type $Ca^{2+}$ channels (Barg *et al*., 2001), whereas replenishment of this pool by mobilization of granules originally residing in a large reserve pool gives rise to the slower component. Interestingly, the initial component can selectively be prevented by intracellular addition of a recombinant peptide corresponding to the loop connecting domains II and III of $Ca_v1.2$ (Wiser *et al*., 1999; Barg *et al*., 2001), suggesting that the assembly of a tight $Ca^{2+}$ channel/insulin granule complex is required for rapid exocytosis in the β cell.

Here we have investigated the role of the L-type $Ca_v1.2$ $Ca^{2+}$ channel for insulin secretion by combining a targeted gene knockout approach with time-resolved insulin release assays and high-resolution single-cell capacitance measurements of exocytosis. Our results suggest that $Ca_v1.2$ $Ca^{2+}$ channels are required for first-phase insulin release and maintenance of systemic glucose tolerance. Collectively, these data raise the interesting possibility that polymorphisms of genes encoding proteins involved in the formation of the exocytotic core/$Ca^{2+}$ channel complex may lead to an impairment of rapid insulin secretion, a hallmark of human type-2 diabetes.

## Results

### *Generation of $\beta Ca_v1.2^{-/-}$ mice*

Mice lacking the $Ca_v1.2$ L-type $Ca^{2+}$ channel die *in utero* before day 15 post-coitum (Seisenberger *et al*., 2000). To circumvent embryonic lethality, the Cre/loxP recombination system was used to selectively inactivate the $Ca_v1.2$ gene in pancreatic β cells (Figure 1A; see Materials and



Published by Oxford University Press

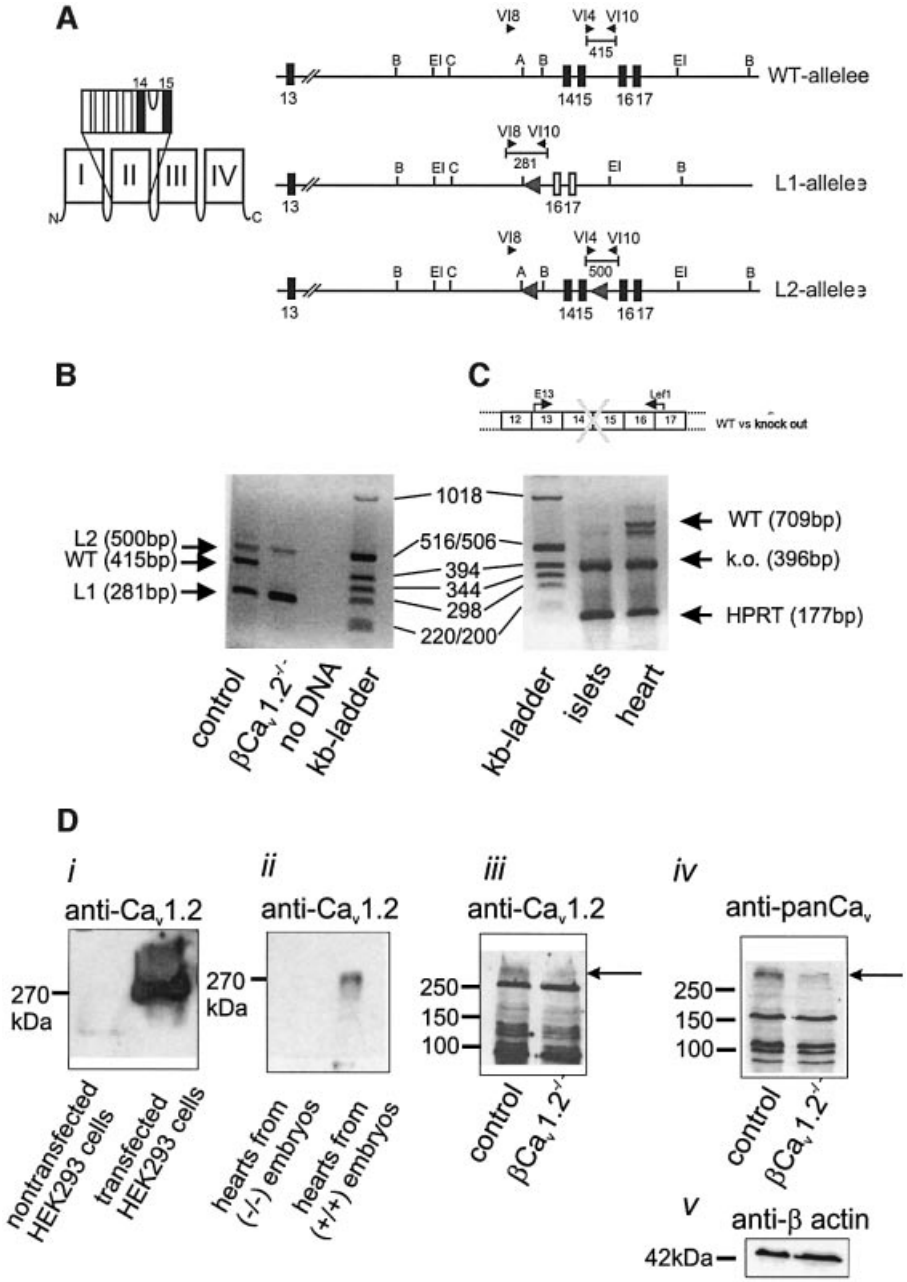


**Fig. 1.** β cell-specific inactivation of the $Ca_v1.2$ gene. (**A**) To the left, a schematic drawing of the location of the transmembrane segments and the pore loop encoded by exons 14 and 15. To the right, the genomic structures of the wild-type and of the mutated $Ca_v1.2$ genes, respectively, are shown. The black arrows indicate the position of the primers used for genotyping and the fragment length of the PCR products. The numbers indicate the exon number. Schematic representation of the wild-type allele, the knockout allele (L1) and the conditional $Ca_v1.2$ (L2) allele, which contains two loxP sites flanking exons 14 and 15. (**B**) PCR analysis of genomic DNA from control, β$Ca_v1.2^{-/-}$ islets and control reaction (no DNA) and kb marker lane as indicated below the lanes. (**C**) RT–PCR analysis of islets and heart from a β$Ca_v1.2^{-/-}$ mouse ($Ca_V1.2^{L1/L2}$/RIP-$Cre^{+/tg}$) and kb marker as indicated. The scheme (top) represents the locations of the primer pair E13 and Lef1 used in RT–PCR (lower). The double band in heart was sequenced. The upper band represents wild-type mRNA, whereas the lower band consists of wild-type mRNA missing 80 bp. Because the control mice are heterozygous, the heart also expresses the L2 gene transcript (396 bp). As an internal standard, the hypoxanthine phosphoribosyl transferase (HPRT) cDNA was amplified together with the $Ca_v1.2$ cDNA. (**D**) Western blots of protein extracts from control islets and β$Ca_v1.2^{-/-}$ islets (as indicated) using a $Ca_v1.2$-specific antibody (iii, top), a pan$Ca_v$-specific antibody (iv) and a β-actin antibody (v, bottom). The specificity of the $Ca_v1.2$ antibody was confirmed using HEK293 cells stably transfected with $Ca_v1.2$ cells (i) and by heart preparations from (+/+) or (–/–) embryos (ii) (Seisenberger *et al.*, 2000). Please note: $Ca_v1.2$ shows an apparently higher mol. wt of 270 kDa in this SDS–PAGE system (11%, low cross-linking).

methods for details). β cell-specific Cre/loxP recombination was achieved by expressing the Cre-recombinase under the control of the rat insulin 2 promoter and was ascertained by PCR analysis using DNA isolated from islets of control and β$Ca_v1.2^{-/-}$ mice (Figure 1B). The islets of β$Ca_v1.2^{-/-}$ mice still contained detectable amounts of the 'floxed' $Ca_v1.2$ gene (L2 allele). This we attribute to contribution of DNA from islet cells not expressing the insulin 2 promoter, i.e. α, δ and PP cells. No Cre-mediated recombination was detectable in heart and lung (data not shown). Islet expression of $Ca_v1.2$ mRNA in β$Ca_v1.2^{-/-}$ mice consisted predominantly of the 'knockout' variety of

$Ca_v1.2$ mRNA and only very low amounts of the wild-type transcript could be detected (Figure 1C). By contrast, the wild-type mRNA was still present in heart (Figure 1C), indicating that Cre-mediated recombination did not occur in this tissue. The successful tissue-selective ablation of $Ca_v1.2$ in β cells was supported by western blot analysis (Figure 1D) using both a $Ca_v1.2$-specific (Diii) and a pan $\alpha_1$ antibody recognizing high voltage-gated $Ca^{2+}$ channels (Div). Equal loading of the gels shown in (Diii) and (Div) was ascertained by staining for β-actin. The specificity of the $Ca_v1.2$ antibody was confirmed using HEK293 cells stably transfected with $Ca_v1.2$ (Di) and by heart preparations from (+/+) or (–/–) embryos (Dii) (mouse line A in Seisenberger *et al.*, 2000). Although both antibodies recognize several proteins, it is clear that a band with the mass expected for $Ca_v1.2$ selectively disappears following knockout of $Ca_v1.2$.

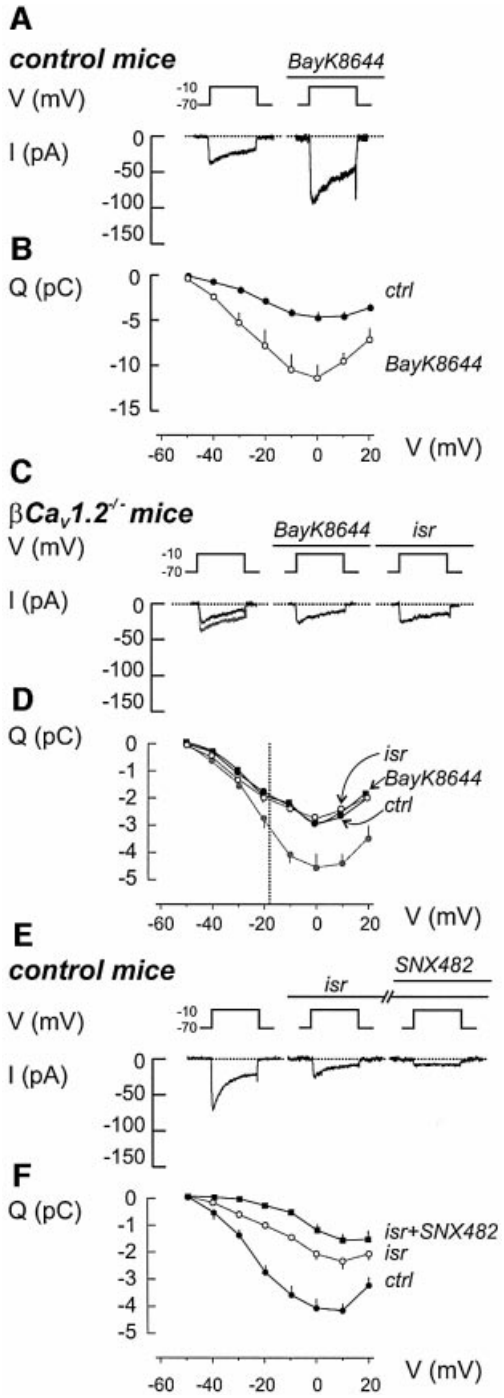


### *Complete and selective loss of L-type $Ca^{2+}$ currents in $\beta Ca_v1.2^{-/-}$ β cells*

We studied the functional consequences of β cell-selective ablation of the $Ca_v1.2$ gene using perforated-patch whole-cell $Ca^{2+}$-current measurements. Figure 2A shows whole-cell $Ca^{2+}$ currents recorded from a control β cell during a 100 ms depolarization from –70 to –10 mV (close to the peak of the β cell action potential; Henquin and Meissner, 1984) under control conditions and after addition of 1 μM specific L-type $Ca^{2+}$ channel agonist BayK8644. The peak $Ca^{2+}$ current elicited by a depolarization to 0 mV in the control β cells (–58 ± 5 pA) was similar to that observed in β cells from NMRI mice (–49 ± 5 pA) under the same experimental conditions (Larsson-Nyrén *et al.*, 2001). The effects of BayK8644 on the integrated $Ca^{2+}$ currents (Q) evoked by depolarizations to voltages (V) between –50 and +20 mV are summarized in Figure 2B. The agonist stimulated the $Ca^{2+}$ current to about the same extent at all voltages, and at –10 mV $Ca^{2+}$ influx increased 2.6 ± 0.6-fold ($P < 0.05$, $n = 5$).

$Ca^{2+}$ currents were reduced in β cells from $\beta Ca_v1.2^{-/-}$ mice. The integrated $Ca^{2+}$ current observed at –10 mV only amounted to 2.4 ± 0.3 pC ($n = 10$), ~55% of the 4.4 ± 0.4 pC ($n = 11$) seen in control β cells. However, it is noteworthy that, up to –30 mV, the amplitude of the $Ca^{2+}$ current was identical in the control and $\beta Ca_v1.2^{-/-}$ β cells. Even at the peak of the β cell action potential (approximately –18 mV; dotted line in Figure 2D), the effects of $Ca_v1.2$ disruption were limited to ~30%. Importantly, BayK8644, as well as the potent L-type $Ca^{2+}$ channel antagonist isradipine (2 μM), were ineffective in these β cells (Figure 2C). The Q–V relationships in $\beta Ca_v1.2^{-/-}$ β cells recorded in the absence and presence of BayK8644 or isradipine are shown in Figure 2D, and are compared with the relationship recorded under control conditions in

**Fig. 2.** $Ca^{2+}$ currents in β cells from control and $\beta Ca_v1.2^{-/-}$ mice. (**A**) Whole-cell $Ca^{2+}$ currents (*I*) during 100 ms depolarizations from –70 to –10 mV (*V*) in the absence (left) and presence (right) of 1 μM BayK8644. The dotted line represents the zero current level. (**B**) Charge (*Q*)–voltage (*V*) relationships recorded in the absence (filled circles) and presence of BayK8644 (open circles). Depolarizations were 100 ms long and went to voltages between –50 and +20 mV. Mean values ± SEM of five experiments. $P < 0.05$ for voltages above –40 mV. (**C** and **D**) As in (A and B) but recordings were conducted on β cells from $\beta Ca_v1.2^{-/-}$ mice. The effects of the L-type channel activator BayK8644 (1 μM) as well as the L-type channel inhibitor isradipine (2 μM) were evaluated. The *Q–V* relationship recorded from control β cells under control conditions has been superimposed (gray). Data represent mean values ± SEM of 10, 10 and 5 experiments carried out under control conditions, in the presence of BayK8644 or after addition of isradipine, respectively. $P < 0.01$ for voltages beyond –20 mV when comparing control currents recorded in $\beta Ca_v1.2^{-/-}$ and control mice. The dotted vertical line indicates the average peak voltage attained during the action potential (approximately –18 mV). (**E** and **F**) as (A and B) but isradipine (2 μM) and SNX482 (0.1 μM) were included sequentially as indicated above the voltage trace. Mean values ± SEM of nine experiments. When comparing currents recorded before and after addition of isradipine, $P < 0.01$ at voltages beyond –30 mV. For currents detected before and after addition of SNX482 and in the continued presence of isradipine, $P < 0.05$ at voltages –30 to 0 mV.

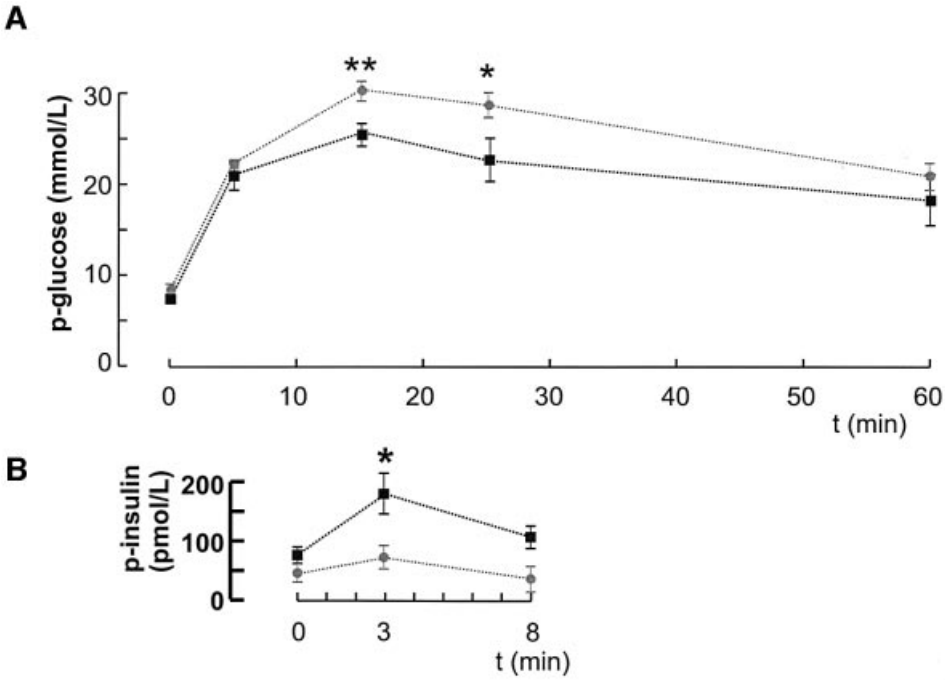


**Fig. 3.** Impaired glucose tolerance and *in vivo* insulin secretion in $\beta Ca_v1.2^{-/-}$ mice. (**A**) Changes in plasma glucose (p-glucose) in response to an intraperitoneal glucose challenge (2 g/kg body weight) applied at time zero in control (black squares) and $\beta Ca_v1.2^{-/-}$mice (gray squares). Data are mean values ± SEM of nine animals for both data sets. (**B**) Plasma insulin levels (p-insulin) measured in control (black squares) and $\beta Ca_v1.2^{-/-}$ mice (gray squares) at 0, 3 and 8 min after glucose injection.

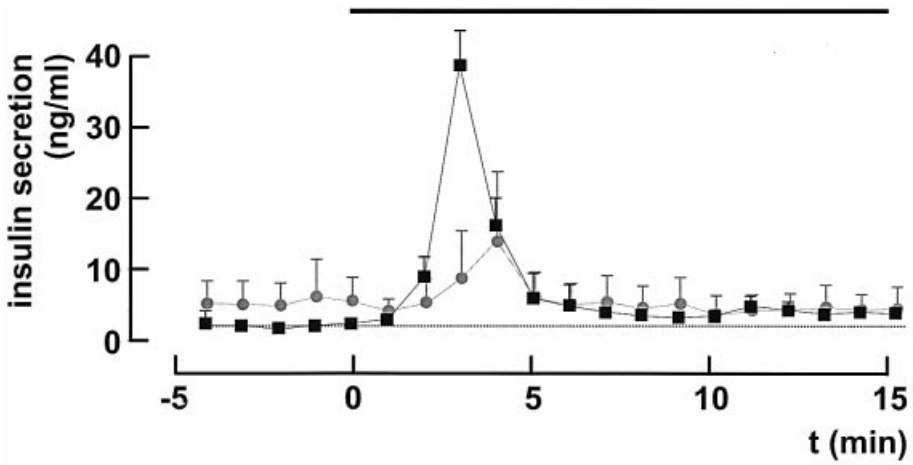


**Fig. 4.** Blunted first-phase insulin secretion in $\beta Ca_v1.2^{-/-}$ pancreata. Insulin release from *in situ* perfused pancreatic glands from control (black squares) and $\beta Ca_v1.2^{-/-}$ mice (gray circles) before and after elevating glucose from 1 to 10 mM (black horizontal bar). The dotted horizontal line corresponds to the pre-stimulatory rate of insulin release in control mice. Data represent mean values ± SEM of four animals in both groups.

control β cells (gray line). Cell capacitance was nearly identical in $\beta Ca_v1.2^{-/-}$ and control β cells (5.9 ± 0.2 and 5.8 ± 0.3 pF, respectively), demonstrating that the smaller $Ca^{2+}$ current in $\beta Ca_v1.2^{-/-}$ β cells indeed reflects a reduced $Ca^{2+}$ channel density.

To confirm the β cell-selective ablation of $Ca_v1.2$, we measured whole-cell $Ca^{2+}$ currents in glucagon-producing α cells. As expected, the amplitude of the $Ca^{2+}$ current in α cells (identified by the presence of a $Na^+$ current activated at physiological membrane potentials; Barg *et al*., 2000) was unaffected in $\beta Ca_v1.2^{-/-}$ mice. The mean charge entry during a 100 ms depolarization to –10 mV amounted to –4.4 ± 0.4 pC ($n$ = 18) and –4.5 ± 0.5 pC ($n$ = 8) in α cells from $\beta Ca_v1.2^{-/-}$ and control mice, respectively (data not shown). The effects of BayK8644 (1 μM) on the α cell $Ca^{2+}$ current in $\beta Ca_v1.2^{-/-}$ mice were tested in four cells and increased the $Ca^{2+}$ current by 58 ± 8% ($P < 0.01$, $n$ = 4; data not shown).

The consequences of ablating $Ca_v1.2$ on the β cell $Ca^{2+}$ current are similar to those obtained using isradipine (Figure 2E). Isradipine blocked the $Ca^{2+}$ current to the same extent at all voltages and the integrated current observed at –10 mV was reduced by 53 ± 6% ($n$ = 9). Nifedipine (20 μM) likewise reduced the β cell $Ca^{2+}$

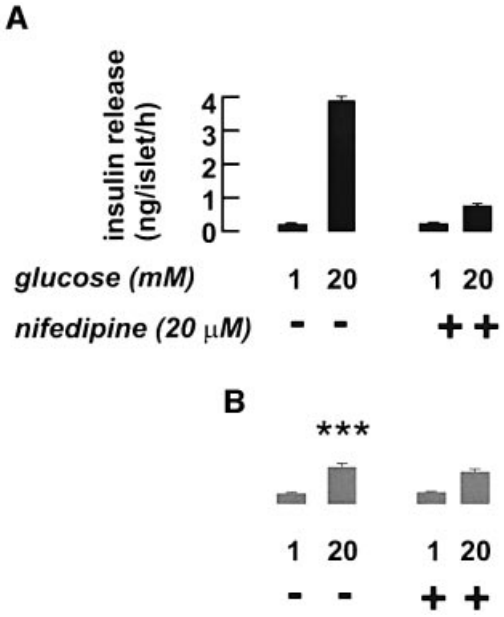


**Fig. 5.** Loss of a nifedipine-sensitive component of insulin release in isolated $Ca_v1.2^{-/-}$ islets. Insulin secretion measured in isolated islets from control (**A**, black bars) and $Ca_v1.2^{-/-}$ mice (**B**, gray bars) in the presence of 1 or 20 mM glucose with or without 20 μM nifedipine as indicated. Data are mean values ± SEM of six experiments. ***$P < 0.001$ versus the same condition in control mice.

current by 51 ± 4% ($n = 5$; data not shown). We also tested the R-type $Ca^{2+}$ channel antagonist SNX482 (Vajna *et al.*, 2001) on the isradipine-resistant component. The action of SNX482 was voltage-dependent and it blocked ⩾60% of the isradipine-resistant component at voltages up to –10 mV. A cocktail of isradipine, SNX482 and the P-/Q-type $Ca^{2+}$ channel inhibitors ω-conotoxin MVIIC (0.5 μM) or ω-agatoxin IVA (0.1 μM) reduced $Ca^{2+}$ current elicited by depolarizations to –10 mV by 97 ± 4% ($n = 4$; data not shown).

### *βCa$_v$1.2$^{-/-}$ mice exhibit impaired glucose tolerance and insulin secretion in vivo*

We next determined the consequences of β cell-selective disruption of the $Ca_v1.2$ gene on systemic glucose homeostasis and insulin release. The β$Ca_v1.2^{-/-}$ mice exhibited a slight hyperglycemia under basal and fasted (6 h) conditions. Fasting glucose levels averaged 6.8 ± 0.4 mM ($n = 8$) and 7.7 ± 0.4 mM ($P < 0.001$, $n = 7$) in control and β$Ca_v1.2^{-/-}$ mice, respectively (data not shown). An intraperitoneal glucose challenge (2 g/kg body weight) in fed mice (Figure 3A) revealed an impaired glucose tolerance in β$Ca_v1.2^{-/-}$ mice, glucose concentrations as high as ~30 mM being attained. This correlated with a slight reduction of basal plasma insulin levels and marked reduction of glucose-induced first-phase insulin secretion (measured 3 min after the glucose challenge) in the β$Ca_v1.2^{-/-}$mice (Figure 3B).

### *Loss of first-phase insulin secretion in βCa$_v$1.2$^{-/-}$ mice in vitro*

To allow comparison between the kinetics of glucose-induced insulin secretion in control and β$Ca_v1.2^{-/-}$ mice, *in situ* pancreatic perfusions were carried out (Figure 4). In control animals, elevating the glucose concentration (from 1 to 10 mM) produced a ~20-fold enhancement of secretion that peaked 3 min after onset of stimulation (compare parts in Figure 3B). In β$Ca_v1.2^{-/-}$ mice, first-phase (<5 min) secretion was inhibited by 78 ± 12% ($P < 0.01$) and the remaining secretory response peaked ~1 min later than in control animals. No difference in insulin secretion between control and β$Ca_v1.2^{-/-}$ mice was observed ⩾5 min after onset of stimulation.

We correlated these observations to insulin secretion *in vitro* using isolated islets. In control mice (Figure 5A), an increase in extracellular glucose from 1 to 20 mM stimulated insulin secretion 16-fold. The L-type $Ca^{2+}$ channel blocker nifedipine (20 μM) had no effect on basal secretion but inhibited glucose-induced release by close to 80%. The R-type channel inhibitor SNX482 (100 nM) likewise failed to affect basal insulin release, but inhibited glucose-elicited insulin secretion by a mere 10% ($n = 6$; data not shown). In agreement with these results, glucose remained capable of stimulating insulin secretion 3.1-fold even in the presence of nifedipine. The latter effect we attribute to $Ca^{2+}$ entry through non-L-type $Ca^{2+}$ channels. In islets from β$Ca_v1.2^{-/-}$ mice (Figure 5B), basal insulin secretion was unaffected, but glucose-induced insulin secretion was much lower than in the control mice and comparable to that seen after blockage of the $Ca^{2+}$ channels with nifedipine (2.7-fold enhancement). As expected, given that $Ca_v1.2$ channels appear to constitute the only L-type $Ca^{2+}$ channels in the β cell (Figure 2C and D), nifedipine had no effect on glucose-induced insulin secretion in the knockout mice. The suppressed insulin secretory capacity in islets from β$Ca_v1.2^{-/-}$ mice could not be attributed to reduced total insulin content, which amounted to 25 ± 1 ng/islet ($n = 13$) and 23 ± 2 ng/islet ($n = 8$) in islets from control and β$Ca_v1.2^{-/-}$ mice, respectively.

### *Intracellular Ca$^{2+}$ handling and electrical activity are unperturbed in β cells from βCa$_v$1.2$^{-/-}$ mice*

The impaired insulin secretory capacity of β$Ca_v1.2^{-/-}$ islets is not attributable to abnormalities of intracellular $Ca^{2+}$ handling (Figure 6A and B) or glucose-induced electrical activity (Figure 6C and D). Basal $[Ca^{2+}]_i$ averaged 103 ± 8 nM ($n = 8$) and 112 ± 12 nM ($n = 8$) in control and β$Ca_v1.2^{-/-}$ islets, respectively. Following stimulation with 10 mM glucose, $[Ca^{2+}]_i$ rose to a peak value of 279 ± 25 nM in control islets and 325 ± 55 nM in islets from the knockout mice. The time-averaged $[Ca^{2+}]_i$ measured both at 10 and 20 mM glucose were likewise not different in the two strains of mice (data not shown). The latency between glucose addition and the initial increase in $[Ca^{2+}]_i$ averaged 257 ± 24 s in control islets and 327 ± 18 s ($P < 0.05$) in β$Ca_v1.2^{-/-}$ islets.

We ascertained that steady-state electrical activity was not significantly affected by ablation of $Ca_v1.2$. In control mice, the membrane potential changed from a resting potential of –62 ± 3 mV ($n = 4$) in the absence of glucose to –17 ± 5 mV (measured at the peak of the action potential) in the presence of 10 mM glucose. The corresponding values in the β cells from β$Ca_v1.2^{-/-}$ mice averaged –64 ± 5 and –19 ± 4 mV ($n = 4$). It is evident that the pattern of action potential firing in β cells from

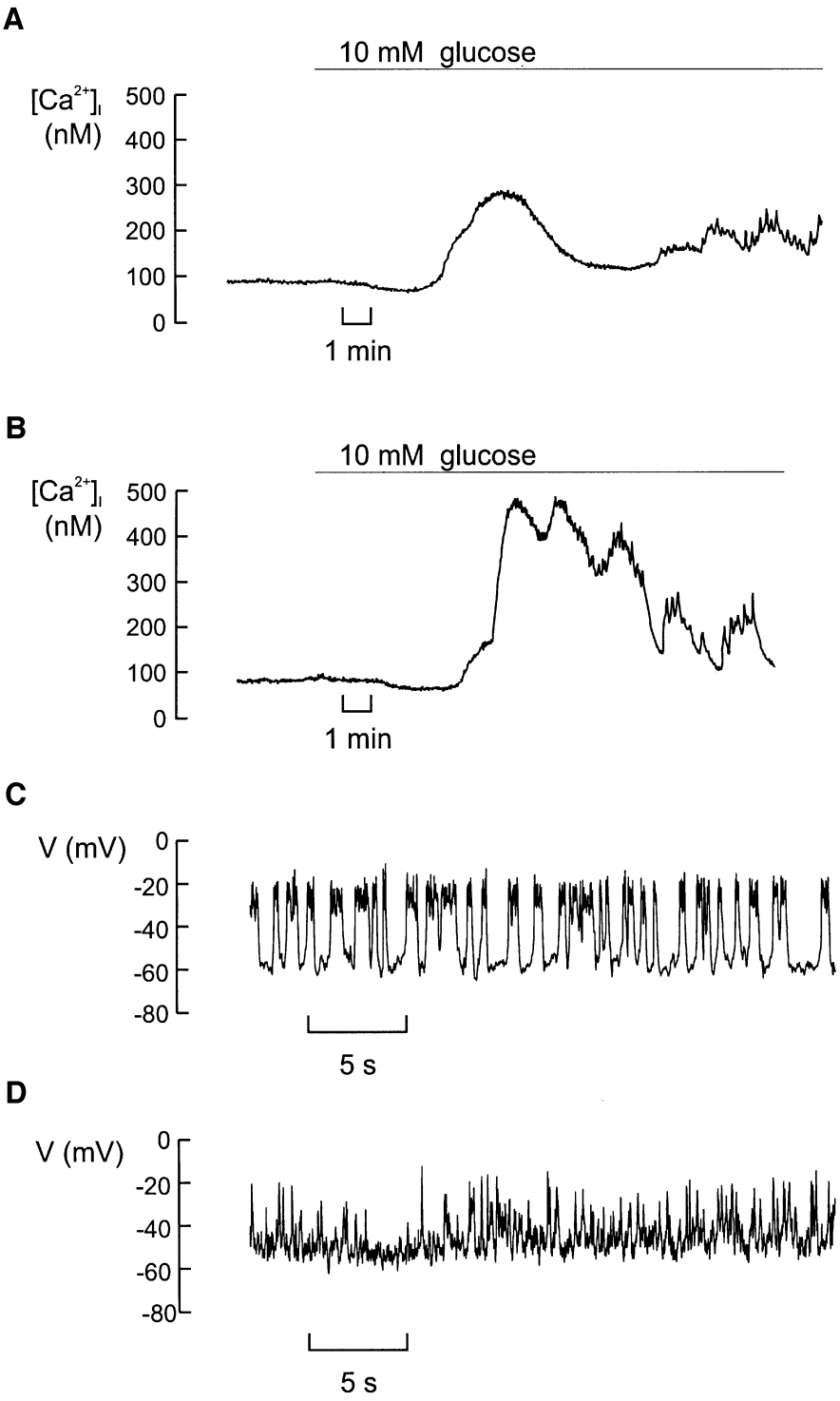


**Fig. 6.** Intracellular $Ca^{2+}$ handling and glucose-induced electrical activity are only moderately affected by disruption of the $Ca_v1.2$ gene. (**A**) Cytoplasmic $Ca^{2+}$ ($[Ca^{2+}]_i$) measured before and after addition of 10 mM glucose in an islet isolated from a control mouse. (**B**) As in (A) but using an islet isolated from a $\beta Ca_v1.2^{-/-}$ mouse. Data are representative of eight recordings in each group. (**C**) Recording of the membrane potential from a β cell in a small cell cluster isolated from control islets exposed to 10 mM glucose at steady state. (**D**) The same as in (C) but in a β cell from a $\beta Ca_v1.2^{-/-}$ mouse. Data are representative of four recordings in both groups that lasted long enough to permit multiple changes of the external solutions (>20 min).

$\beta Ca_v1.2^{-/-}$ mice was somewhat different from that observed in the control mice in not being grouped to short bursts. It might seem surprising that $Ca_v1.2$ ablation had no effect on the peak voltage of the action potential given that the peak $Ca^{2+}$ current was reduced by ~30% at –20 mV (Figure 2D). However, several processes in addition to the $Ca^{2+}$-current amplitude influence the shape of the action potential. These include, for example, the magnitude of the resting and voltage-gated $K^+$ conductances.

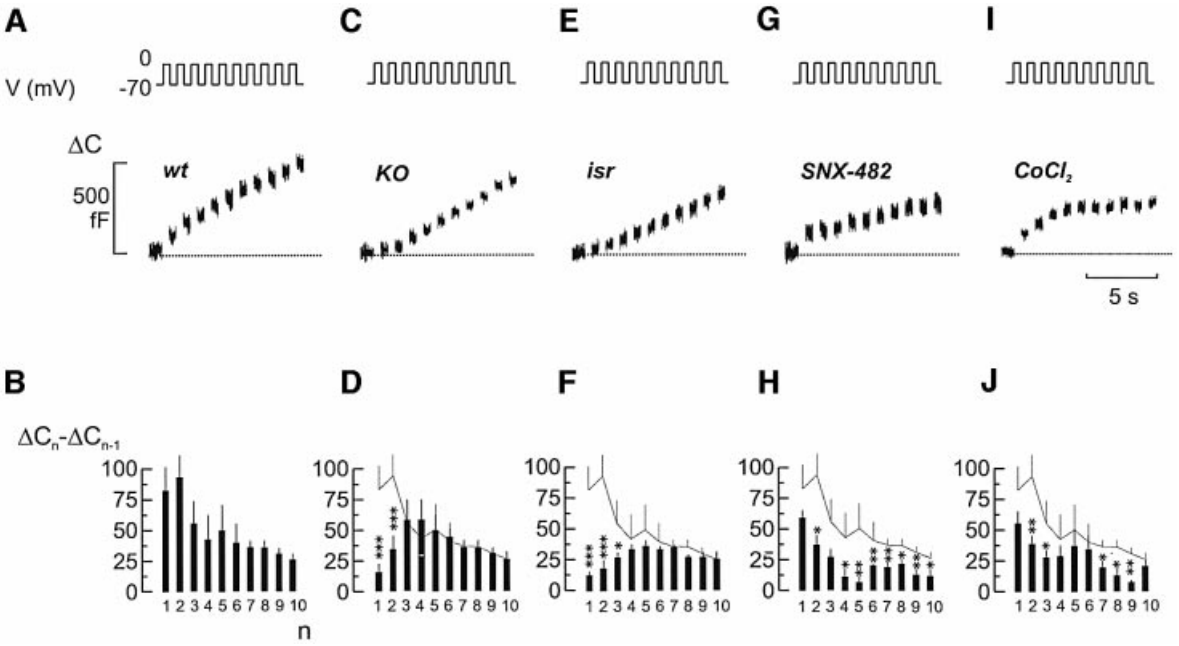


**Fig. 7.** Loss of rapid exocytosis in $\beta Ca_v1.2^{-/-}$ β cells. (**A**) Increase in cell capacitance (ΔC, lower) elicited by a train of ten 500 ms depolarizations from –70 to 0 mV (V, upper). The dotted line indicates the pre-stimulatory level. (**B**) Increment in cell capacitance by each depolarization ($\Delta C_n - \Delta C_{n-1}$) displayed against pulse number ($n$). Data are mean values ± SEM of nine experiments. (**C** and **D**) The same as in (A and B) but using a β cell obtained from a $\beta Ca_v1.2^{-/-}$ mouse. Data are mean values ± SEM of 15 experiments. (**E** and **F**) As in (A and B) but in the presence of 2 μM isradipine. Data are mean values ± SEM of eight experiments. (**G** and **H**) As in (A and B) but in the presence of 0.1 μM SNX482. Data are mean values ± SEM of seven experiments. (**I** and **J**) As in (A and B) but in the presence of 0.5 mM $Co^{2+}$. Data are mean values ± SEM of 11 experiments. In (D, F, H and J), the superimposed gray line denotes the data in control β cells from (A). ***$P < 0.001$, **$P < 0.01$ and *$P < 0.05$ versus responses in the control β cells (gray line).

### *Loss of rapid $Ca^{2+}$-dependent exocytosis in β cells from $\beta Ca_v1.2^{-/-}$ mice*

The mild consequences of ablating $Ca_v1.2$ in β cells on intracellular $Ca^{2+}$ suggest that impaired glucose tolerance and insulin secretion may result from direct interference with the exocytotic apparatus. Indeed, it has been shown previously that $Ca_v1.2$ $Ca^{2+}$ channels co-assemble with fusion proteins including synaptotagmin, syntaxin and SNAP-25 (Wiser *et al*., 1999; Ji *et al*., 2002). We used cell capacitance measurements to study the kinetics of depolarization-evoked exocytosis in single β cells from control and $\beta Ca_v1.2^{-/-}$ mice. Figure 7A shows changes in cell capacitance in response to a train of ten 500 ms depolarizations. The data of a total of nine experiments are summarized in Figure 7B. Typically, the capacitance increase per pulse decreased during the train, from 80 to 100 fF in response to the initial depolarizations to a steady-state rate of 25 fF/pulse. This behavior is expected if the cell contains a limited pool of releasable granules, which are gradually depleted during repetitive stimulation (Neher, 1998; Barg *et al*., 2000, 2001, 2002). When the same experiments were conducted in β cells from $\beta Ca_v1.2^{-/-}$ mice (Figure 7C and D), exocytosis in response to the initial depolarizations was markedly reduced whereas that elicited later during the train was not affected. The $Ca^{2+}$ current elicited by the depolarizations was reduced to an equal extent (~45%) throughout the train (data not shown). The acute effects of applying the L-type $Ca^{2+}$ channel antagonist isradipine were identical to those resulting from $Ca_v1.2$ disruption (Figure 7E and F). By contrast, inhibition of R-type $Ca^{2+}$ channels with SNX482, which reduced the $Ca^{2+}$ current by ~25%, affected late exocytosis but had no significant effect on the response to the first depolarization (Figure 7G and H). The differential effects of selective L- and R-type channel inhibition on rapid and sustained exocytosis, respectively, are at variance with the effect of the non-selective $Ca^{2+}$ channel blocker $Co^{2+}$ (0.5 mM), which inhibited $Ca^{2+}$ entry by ~50% (i.e. the same as that produced by ablation of $Ca_v1.2$), and reduced exocytosis to an equal extent (45 ± 6%; Figure 7I and J) throughout the train.

## Discussion

### *General considerations*

Here we have studied the effects of ablating the L-type $Ca^{2+}$ channel gene $Ca_v1.2$ *in vivo*, at the whole-organ level, in isolated islets and individual islet cells. The combination of techniques makes it possible to correlate the consequences of a single-cell defect on the complex systems physiology of insulin release and plasma glucose homeostasis. The genetic model we have chosen strictly depends on the comparison of litter-matched animals of a control group ($Ca_v1.2^{+/L2}$/RIP-$Cre^{+/tg}$ resulting in the genotype $Ca_v1.2^{+/L1}$/RIP-$Cre^{+/tg}$ only in the β cells) and of a knockout group ($Ca_v1.2^{L1/L2}$/RIP-$Cre^{+/tg}$ resulting in the genotype $Ca_v1.2^{L1/L1}$/RIP-$Cre^{+/tg}$ only in the β cells). These animals are identical with the exception of one functional $Ca_v1.2$ allele in the control group. Therefore, we compare animals with two knockout alleles with those with one wild-type allele, allowing us to establish the specific function of $Ca_v1.2$. Careful analysis of the L-type

$Ca^{2+}$-current densities in embryonic cardiomyocytes for all three genotypes and two differently constructed mouse lines (stop codon in exon 3 versus deletion of exons 14/15 and stop in 16) failed to detect significant differences between (+/+) and (+/–) cells (Seisenberger *et al*., 2000). We have also analyzed mice in which the $Ca_v1.2$ channel was specifically deleted in smooth muscle cells. $Ca_v1.2$ current densities were identical in litter-matched animals for the genotypes (+/–) or (+/+) (N.Klugbauer and F.Hofmann, unpublished data). These considerations indicate that a gene dose effect does not account for the present results.

In the following, we will consider the molecular identity of the L-type $Ca^{2+}$ channel in the pancreatic β cell, the importance of the L-type $Ca_v1.2$ channel for systemic glucose control and first-phase insulin secretion, as well as the functional roles fulfilled by other $Ca^{2+}$ channel subtypes expressed in β cells. Finally, we discuss the possibility that defects of the release machinery and/or $Ca^{2+}$ entry contribute to the impaired insulin secretion seen in human type-2 diabetes.

### *Mouse L-type $Ca^{2+}$ channel variety expressed in β cells is $Ca_v1.2$*

The present data unequivocally establish the central role of $Ca_v1.2$ L-type $Ca^{2+}$ channels in insulin secretion. Previous studies have indicated that $Ca_v1.3$ ($\alpha1_D$) might be of importance in insulin release (Yang *et al*., 1999; Namkung *et al*., 2001). However, the finding that the entire DHP-sensitive $Ca^{2+}$ current is lost following inactivation of the $Ca_v1.2$ gene reinforces our previous immunochemical and electrophysiological data that $Ca_v1.2$ is the only L-type $Ca^{2+}$ channel variety expressed in mouse β cells (Barg *et al*., 2001). In addition to the L-type $Ca^{2+}$ channels, mouse β cells also express R- and P/Q-type $Ca^{2+}$ channels. Although the L-type current component accounts for only ~50% of the total $Ca^{2+}$ current, its inhibition reduces glucose-induced insulin secretion *in vitro* by 80% and nearly abolishes insulin release *in vivo*. Thus, it appears that the conduit of $Ca^{2+}$ entry determines the biological efficacy of the ion and that influx through L-type $Ca^{2+}$ channels is more tightly coupled to insulin secretion than that occurring via P/Q- and R-type $Ca^{2+}$ channels.

### *$Ca_V1.2$ $Ca^{2+}$ channels are required for first-phase insulin secretion and rapid exocytosis in pancreatic β cells*

We have previously demonstrated that $Ca_v1.2$ $Ca^{2+}$ channels functionally associate with insulin granules in the β cells, and that the loop connecting the second and third homologous domains physically tethers the channel to components of the exocytotic core complex (Wiser *et al*., 1999). It is therefore pertinent that the effects of isradipine and genetic ablation of $Ca_v1.2$ are indistinguishable from those of intracellular application of the synprint peptide (Barg *et al*., 2001). We propose that in $\beta Ca_v1.2^{-/-}$ mice, the $Ca_v1.2$/granule complex is disrupted, leading to selective suppression of fast exocytosis. We emphasize that the effects of inhibition of L-type $Ca^{2+}$ channels or ablation of the $Ca_v1.2$ gene are not simply attributable to the fact that the whole-cell $Ca^{2+}$ current is reduced by 50%. This possibility can be discarded by the finding that addition of the non-selective $Ca^{2+}$ channel blocker $Co^{2+}$ (0.5 mM), which reduces the total whole-cell $Ca^{2+}$ current (i.e. that flowing through both L- and non-L-type $Ca^{2+}$ channels) by 50%, does not affect the release kinetics but simply reduces the amplitude of the responses observed during the train by ~50%.

The role of the non-L-type $Ca^{2+}$ channels in β cell exocytosis remains enigmatic, but it is worth pointing out that a DHP-resistant component of insulin secretion can be detected both in the insulin-release experiments (Figure 5) as well as the capacitance measurements (Figure 7). It is possible that non-L-type $Ca^{2+}$ channels fulfill functions in the β cells other than initiation of exocytosis. For example, they may play a role in the refilling of the readily releasable pool of granules by mobilizing reserve granules. This would be consistent with the finding that whereas exocytosis elicited by the two first pulses during a train of ten 500 ms depolarizations is strongly inhibited in β cells from $\beta Ca_v1.2^{-/-}$ mice and in control β cells exposed to the L-type $Ca^{2+}$ channel inhibitor isradipine (Figure 7A–F), exocytosis during the latter part of the train is unaffected. Indeed, the R-type $Ca^{2+}$ channel blocker SNX482 exerts its strongest effect on late exocytosis (Figure 7H). In addition, influx of $Ca^{2+}$ through non-L-type $Ca^{2+}$ channels may regulate exocytosis of GABA-containing synaptic-like microvesicles (SLMV; the presence of which has been documented in β cells; Reetz *et al*., 1991) rather than the large insulin-containing secretory granules (compare with Takahashi *et al*., 1997). We have ascertained that exocytosis of SLMVs only contributes ~1% of the total capacitance (M.Braun, A.Wendt and P.Rorsman, manuscript in preparation) increase. It is therefore safe to conclude that the data presented in this study reflect exocytosis of insulin-containing large dense core vesicles. Finally, non-L-type $Ca^{2+}$ channels may not be important for exocytosis, but rather in the generation of glucose-induced electrical activity (Pereverzev *et al*., 2002) or gene expression (Wang *et al*., 2002).

### *$Ca^{2+}$ signaling is unperturbed in $\beta Ca_v1.2^{-/-}$ mice*

Surprisingly, given the strong effects on insulin secretion, ablation of $Ca_v1.2$ had no detectable effects on intracellular $Ca^{2+}$ signaling except that the glucose-induced increase in cytoplasmic $Ca^{2+}$ was delayed by ~1 min relative to that observed in control β cells. The latter effect nicely echoes the slower time-course of insulin release observed *in situ* (~1 min; Figure 4). Possibly, the latter observations are the consequence of L-type $Ca^{2+}$ channels contributing to the initiation of electrical activity in the β cell (Ribalet and Beigelman, 1981).

Why are measured $Ca^{2+}$ concentrations unchanged in $\beta Ca_v1.2^{-/-}$ β cells? The preservation of normal $Ca^{2+}$ signaling is unexpected in view of previous data showing that glucose-induced increases in cytoplasmic $Ca^{2+}$ concentration are suppressed following the addition of L-type $Ca^{2+}$ channel blockers such as nifedipine (Rosario *et al*., 1993). This may result from a compensatory up-regulation of non-L-type $Ca^{2+}$ channels, as suggested by the finding that the peak $Ca^{2+}$ current measured at –20 mV in $Ca_v1.2^{-/-}$ β cells is 50% larger than that observed in control β cells exposed to isradipine (compare Figure 2D, black circles with F, white circles). In fact, the reduction of the whole-cell $Ca^{2+}$ current in the knockout mice was limited to ~30% at voltages up to –20 mV, i.e. the range of voltages

covered by the action potential. This makes the strong inhibition of insulin secretion (~80%; Figures 3–5) even more remarkable and provides additional arguments that exocytosis in the β cell is tightly coupled to $Ca^{2+}$ entry through $Ca_v1.2$.

We emphasize that microfluorimetry reports the global intracellular $Ca^{2+}$ concentration ($[Ca^{2+}]_i$) within the β cell. We have previously documented the existence of steep $Ca^{2+}$ gradients in mouse pancreatic β cells and these are not resolved in the present recordings of $[Ca^{2+}]_i$ in intact pancreatic islets. Our failure to detect any gross abnormalities in cellular $Ca^{2+}$ signaling therefore does not exclude the possibility that $[Ca^{2+}]_i$ at the release sites is affected. The significance of microdomains of high $[Ca^{2+}]_i$ close to the release sites is illustrated by the finding that whereas glucose-induced insulin secretion is nearly abolished in the presence of nifedipine (Figure 5), exocytosis during the latter part of the train of voltage–clamp depolarizations is hardly affected (Figure 7E and F). This apparent discrepancy we attribute to the fact that the stimulus used for the capacitance measurements (trains of 500 ms depolarizations to 0 mV) is much stronger than that normally triggering insulin secretion (50 ms action potentials to ~15 mV; Atwater *et al*., 1979). During the train of depolarizations, $[Ca^{2+}]_i$ equilibrates in the β cell (Bokvist *et al*., 1995) and rises sufficiently throughout the cell to initiate exocytosis of granules that are not in the immediate vicinity of the $Ca^{2+}$ channels. This does not occur during the brief action potentials when exocytotic levels of $[Ca^{2+}]_i$ ($\geqslant$10 μM) are only attained close to the $Ca^{2+}$ channels (Barg *et al*., 2001, 2002).

### *Does human type-2 diabetes result from defective assembly of $Ca^{2+}$ channels and secretory granules?*

It is tempting to consider the significance of these findings to human type-2 diabetes. Like the $\beta Ca_v1.2^{-/-}$ mice, early cases of type-2 diabetes exhibit mild basal hyperglycemia, impaired glucose tolerance and lack of first-phase insulin secretion (UKPDS16, 1995). We are not implying that loss-of-function mutations of the $Ca_v1.2$ gene cause diabetes. However, polymorphisms that result in subtle changes in gating of the $Ca^{2+}$ channel or its ability to interact with the exocytotic machinery (Nagamatsu *et al*., 1999; Wiser *et al*., 1999; Zhang *et al*., 2002) can be envisaged to result in impaired insulin secretion. The significance of such interactions is illustrated by the fact that whereas the SNARE proteins SNAP-25 and syntaxin1A inhibit the L-type $Ca^{2+}$ channel when expressed individually, channel activity is actually stimulated when these proteins are co-expressed (Wiser *et al*., 1999; Ji *et al*., 2002). Interestingly, SNARE protein expression is reduced in the GK rat model of human type-2 diabetes (Nagamatsu *et al*., 1999; Zhang *et al*., 2002) and several proteins known to be important for the anchoring of the insulin granules to the $Ca^{2+}$ channels localize to chromosomal regions linked to human type-2 diabetes. These include the insulin granule proteins synaptotagmins 5 and 7 (Haeger *et al*., 1998; Norman *et al*., 1998; Pratley *et al*., 1998), putative $Ca^{2+}$ sensors in β cell exocytosis (Ji *et al*., 2002), the granular fusion protein VAMP-2/synaptobrevin-2 (Regazzi *et al*., 1995; Parker *et al*., 2001; Lindgren *et al*., 2002) and the plasma membrane-associated fusion protein SNAP-25 (Imperatore *et al*., 1998; Ji *et al*., 2002). Indeed, a single nucleotide polymorphism in the gene encoding syntaxin1A has recently been found to associate with human type-2 diabetes (Tsunoda *et al*., 2001). $Ca^{2+}$ channels and proteins involved in exocytosis therefore deserve to be regarded as interesting candidate genes in genetic studies of type-2 diabetes. We point out that the functional consequences of the polymorphisms must be small as we are not born with type-2 diabetes. This suggests that the changes in protein function resulting from the polymorphisms only become significant when combined with other β cell abnormalities such as age-dependent reduction in glucose metabolism (due to accumulating mitochondrial mutations; Maechler and Wollheim, 2001) with resultant impairment of electrical activity and $Ca^{2+}$ entry. This concept is indeed entirely compatible with the current view that diabetes results from a combination of genetic factors, age and environmental factors (McCarthy and Froguel, 2002). Genes encoding proteins involved in exocytosis (SNARE proteins as well as $Ca^{2+}$ channels) should accordingly be considered as candidate genes in future studies of the genetics of type-2 diabetes.

## Materials and methods

### *Conditional inactivation of the $Ca_v1.2$ gene in pancreatic β cells*

As described previously (Seisenberger *et al*., 2000), two different $Ca_v1.2$ alleles were generated by Cre-mediated recombination in ES cells (L1 and L2; Figure 1A). In L1, exons 14 and 15 that encode the IIS5 and IIS6 transmembrane segments and the pore loop in domain II were deleted. In addition, this deletion causes incorrect splicing from exon 13 to an intron upstream of exon 16, and thereby generates a premature stop codon in exon 16 and a loss-of-function allele. L2 contains the 'floxed' exons 14 and 15, and encodes a functional $Ca_v1.2$ gene. To generate β cell-specific $Ca_v1.2$-deficient mice, the $Ca_v1.2^{+/L1}$ mouse (i.e. a mouse carrying one L1 allele and one wild-type allele) was crossed with a mouse expressing the Cre-recombinase under the control of the rat insulin 2 promoter ($RipCre^{+/tg}$) (Postic *et al*., 1999). The resulting $Ca_v1.2^{+/L1}$,$RipCre^{+/tg}$ mice were then mated with $Ca_v1.2^{L2/L2}$ mice (i.e. mice homozygous for the L2 allele) to obtain the β cell-specific knockout $Ca_v1.2^{L1/L2}$,$RipCre^{+/tg}$ (i.e. $\beta Ca_v1.2^{-/-}$ mice) and control animals ($Ca_v1.2^{+/L2}$,$RipCre^{+/tg}$). Both lines were viable and showed no gross abnormalities. Genotyping was performed using primers VI4 (5′-TGGCCCCTAAGCAATGA-3′), VI8 (5′-AGGGGTGTTCAGAGCAA-3′) and VI10 (5′-CCCCAGCCAA-TAGAATGCCAAT-3′). The background mouse strain was C57BL/6.

### *Isolation of pancreatic islets*

Mice (3–4 months old) were killed by cervical dislocation, the pancreas quickly excised and pancreatic islets isolated by standard collagenase digestion (Salehi *et al*., 1999). The surgical procedures used in the *in vitro* and *in vivo* studies were approved by the ethical committee at Lund University, the Regierung von Oberbayern or by the Veterinary Office of the canton of Geneva.

### *DNA isolation from islets and PCR analysis*

Islets were digested for 5 min at 55°C in 19 μl of buffer containing 50 mM Tris pH 8.0, 20 mM NaCl, 1 mM EDTA, 1% SDS and 1 mg/ml proteinase K. Proteinase K was subsequently inactivated by increasing the temperature of the digest to 95°C for 5 min. The digest (0.1 μl) was taken for PCR analysis using the $Ca_v1.2$-specific primers VI4, VI8 and VI10.

### *RT–PCR on mRNA of islets*

Freshly prepared islets were cultured overnight in RPMI 1640 medium (Gibco™) at 37°C. PolyA mRNA was isolated using Dynabeads Oligo $(dT)_{25}$ (Dynal Biotech, Oslo, Norway). The following buffers were used: GTC buffer [4 M guanidine thiocyanate, 20 mM Na acetate pH 5.4, 0.1 mM DTT, 0.5% lauroyl sarcosinat (w/v), 6.5 μl/ml mercaptoethanol],

binding buffer (100 mM Tris–HCl pH 8.0, 20 mM EDTA, 400 mM LiCl) and washing buffer (10 mM Tris–HCl pH 8.0, 0.15 M LiCl, 1 mM EDTA). The mRNA was eluted with DEPC-treated water. Random hexamer primers and Superscript Reverse Transkriptase II (Life Technologies) were used for cDNA synthesis. The following primers were used: for amplifying $Ca_v1.2$ (E13 5′-ACAGCCAATAAAG-CCCTCCT-3′ and Lef 1 5′-GGCTTCTCCATCACCTCCTGTT-3′), for HPRT (QG 197 5′-GTAATGATCAGTCAACGGGGGAC-3′ and QG 198 5′-CCAGCAAGCTTGCAACCTTAACCA-3′).

### Western blot analysis

Approximately 900 islets of control and $\beta Ca_v1.2^{-/-}$ mice were cultured in RPMI 1640 for 48 h at 37°C. Thereafter, the islets were homogenized after one freeze–thaw cycle in a hypotonic buffer (20 mM $K_2HPO_4$/$KH_2PO_4$ pH 7.2, 1 mM EDTA) containing protease inhibitors [1 mM benzamidine, 0.1 mM PMSF and Protease Inhibitor Cocktail (1:500; Sigma)]. The homogenates (40 μg protein) were separated on an 11% SDS–PAGE (lower crosslinking with 0.2% bis-acrylamide). Peptides were blotted on a PVDF membrane (Millipore) and probed with a $Ca_v1.2$-(Chemicon) and a pan$Ca_v$-specific antibody (Calbiochem). Equal loading of the slots was ascertained using a monoclonal β-actin antibody (Abcam). Antibodies were visualized by the ECL system (NEN).

### Glucose and insulin measurements

In the *in vivo* studies, glucose [11.1 mmol (equal to 2 g)/kg body weight] was dissolved in 0.9% NaCl and delivered by intraperitoneal injection. Blood sampling, detection of plasma insulin by RIA and enzymatic determination of plasma glucose concentrations were performed as described previously (Salehi *et al*., 1999). *In situ* pancreatic perfusions were performed as detailed in Maechler *et al*. (2002), except that the basal and stimulatory glucose concentrations in the perfusate were 1 and 10 mM, respectively. Insulin release *in vitro* was measured in batch incubations. Briefly, freshly isolated islets were pre-incubated for 30 min at 37°C in a Krebs–Ringer bicarbonate buffer pH 7.4 supplemented with 7 mM glucose, 10 mM HEPES and 0.1% bovine serum albumin, and gassed with 95% $O_2$ and 5% $CO_2$. Groups of 10 islets were then incubated in 1 ml for 60 min at 37°C in KRB supplemented with glucose and nifedipine as specified. Total insulin islet content was determined by extraction with acidic ethanol and insulin was assayed by RIA.

### Electrophysiology

Isolated islets (see above) were dissociated into single cells by shaking in $Ca^{2+}$-free medium. Insulin-secreting β cells and glucagon-producing α cells were identified electrophysiologically by the absence and presence, respectively, of $Na^+$ currents at physiological membrane potentials (Barg *et al*., 2000). The measurements were conducted using an EPC-7 patch–clamp amplifier in conjunction with the software Pulse (version 8.53; HEKA Elektronik, Lambrecht/Pfalz, Germany). Whole-cell $Ca^{2+}$ currents and glucose-induced electrical activity were recorded from metabolically intact cells using the perforated-patch whole-cell approach (Renström *et al*., 1996). Exocytosis was monitored using standard whole-cell measurements that allow control of the cytosol, by recordings of cell capacitance using the sine+DC mode of the lock-in amplifier included in the Pulse software suite. The extracellular bath solution contained (in mM) 138 NaCl, 5.6 KCl, 2.6 $CaCl_2$, 1.2 $MgCl_2$, 5 glucose (unless otherwise indicated) and 5 HEPES (pH 7.4 with NaOH). For the recordings of the whole-cell $Ca^{2+}$ currents, 20 mM NaCl was equimolarly replaced by the $K^+$ channel blocker TEA-Cl. The pipette solution in the perforated-patch recordings of membrane potential contained (in mM) 76 $K_2SO_4$, 10 NaCl, 10 KCl, 1 $MgCl_2$, 5 HEPES (pH 7.35 with KOH) and 0.24 mg/ml amphotericin B (Renström *et al*., 1996). For the whole-cell $Ca^{2+}$ current recordings, the $K^+$ salts in the pipette solution were replaced by the corresponding $Cs^+$ salts. The intracellular medium used in the capacitance measurements consisted of (in mM): 125 Cs glutamate, 10 CsCl, 10 NaCl, 1 $MgCl_2$, 5 HEPES, 3 Mg ATP, 0.1 cAMP and 0.05 EGTA (pH 7.2 with CsOH). The dihydropyridines nifedipine, isradipine (Pfizer) and BayK8644 were prepared as stock solutions in DMSO (final concentration ≤0.1%). The R-type blocker SNX482 (Peptide Institute Inc., Osaka, Japan) was dissolved directly in the extracellular medium. All other reagents were from Sigma. Effects of agonists and antagonists were determined in the steady state. The bath (~1.5 ml) was continuously perfused (6 ml/min) and the temperature maintained at ~32°C.

### Microfluorimetry

$[Ca^{2+}]_i$ in intact pancreatic islets was measured by dual-wavelength microfluorimetry using fura-2 and a D104 PTI microfluorimetry system (Monmouth Junction, NJ). The temperature of the experimental chamber was +32°C. Procedures for loading and calibration of the fluorescence signal were as detailed in Olofsson *et al*. (2002).

### Data analysis

Data are given as mean values ± SEM. Statistical significances were evaluated by either ANOVA followed by Dunnet's ad hoc tests for unpaired comparisons, or by paired Student's *t*-test when comparing data obtained in the same cell.

## Acknowledgements

We thank Mrs K.Borglid, Mrs B-M.Nilsson and Mrs S.Paparisto for expert technical assistance. and Dr Cecilia Lindgren for help with diabetes genetics. Supported by the JDRF, the Swedish Research Council (grant nos 08647, 13509, 12234), the Swedish Diabetes Association, the NovoNordisk Foundation, the European Commission (HPRN-CT-2000-00082), the Deutsche Forschungsgemeinschaft, Fond der Chemischen Industrie, Swiss National Science Foundation (grant no 32-66907.01) and the Swiss Federal Office for Education and Science (grant no 01.0260).

## References

Ashcroft,F.M. and Rorsman,P. (1989) Electrophysiology of the pancreatic β-cell. *Prog. Biophys. Mol. Biol.,* **54**, 87–143.

Atwater,I., Dawson,C.M., Ribalet,B. and Rojas,E. (1979) Potassium permeability activated by intracellular calcium ion concentration in the pancreatic β cell. *J. Physiol.*, **288**, 575–588.

Barg,S., Galvanovskis,J., Göpel,S., Rorsman,P. and Eliasson,L. (2000) Tight coupling between electrical activity and exocytosis in mouse glucagon-secreting α-cells. *Diabetes*, **49**, 1500–1510.

Barg,S. *et al*. (2001) Fast exocytosis with few $Ca^{2+}$ channels in insulin-secreting mouse pancreatic B cells. *Biophys. J.*, **81**, 3308–3323.

Barg,S., Eliasson,L., Renström,E. and Rorsman,P. (2002) A subset of 50 secretory granules in close contact with l-type $ca^{2+}$ channels accounts for first-phase insulin secretion in mouse β-Cells. *Diabetes*, **51**, S74–S82.

Bokvist,K., Eliasson,L., Ämmälä,C., Renström,E. and Rorsman,P. (1995) Co-localization of L-type $Ca^{2+}$ channels and insulin-containing secretory granules and its significance for the initiation of exocytosis in mouse pancreatic B-cells. *EMBO J.*, **14**, 50–57.

Bratanova-Tochkova,T.K. *et al*. (2002) Triggering and augmentation mechanisms, granule pools, and biphasic insulin secretion. *Diabetes,* **51**, S83–S90.

Curry,D.L., Bennett,L.L. and Grodsky,G.M. (1968) Dynamics of insulin secretion by the perfused rat pancreas. *Endocrinology*, **83**, 572–584.

Eliasson,L., Renstrom,E., Ding,W.G., Proks,P. and Rorsman,P. (1997) Rapid ATP-dependent priming of secretory granules precedes $Ca^{2+}$-induced exocytosis in mouse pancreatic B-cells. *J. Physiol.*, **503**, 399–412.

Gilon,P., Yakel,J., Gromada,J., Zhu,Y., Henquin,J.C. and Rorsman P. (1997) G protein-dependent inhibition of L-type $Ca^{2+}$ currents by acetylcholine in mouse pancreatic B-cells. *J. Physiol.*, **499**, 65–76.

Hager,J. *et al*. (1998) A genome-wide scan for human obesity genes reveals a major susceptibility locus on chromosome 10. *Nat. Genet.*, **20**, 304–308.

Henquin,J.C. and Meissner,H.P. (1984) Significance of ionic fluxes and changes in membrane potential for stimulus–secretion coupling in pancreatic β-cells. *Experientia*, **40**, 1043–1052.

Imperatore,G., Hanson,R.L., Pettitt,D.J., Kobes,S., Bennett,P.H. and Knowler,W.C. (1998) Sib-pair linkage analysis for susceptibility genes for microvascular complications among Pima Indians with type 2 diabetes. Pima Diabetes Genes Group. *Diabetes*, **47**, 821–830.

Ji,J,. Yang,S.N., Huang,X., Li,X., Sheu,L., Diamant,N., Berggren,P-O. and Gaisano,H.Y. (2002) Modulation of L-type $Ca^{2+}$ channels by distinct domains within SNAP-25. *Diabetes*, **51**, 1425–1436.

Larsson-Nyrén,G., Sehlin,J., Rorsman,P. and Renstrom,E. (2001) Perchlorate stimulates insulin secretion by shifting the gating of L-type $Ca^{2+}$ currents in mouse pancreatic B-cells towards negative potentials. *Pflugers Arch.*, **441**, 587–595.

Lindgren,C.M. *et al*. (2002) Contribution of known and unknown susceptibility genes to early-onset diabetes in Scandinavia: evidence for heterogeneity. *Diabetes*, **51**, 1609–1617.

Maechler,P. and Wollheim,C.B. (2001) Mitochondrial funtion in normal and diabetic β-cells *Nature*, **414**, 807–812.

Maechler,P., Gjinovci,A. and Wollheim,C.B. (2002) Implication of glutamate in the kinetics of insulin secretion in rat and mouse perfused pancreas. *Diabetes*, **51**, (Suppl. 1), S99–S102.

McCarthy,M.I. and Froguel,P. (2002) Genetic approaches to the molecular understanding of type 2 diabetes. *Am. J. Physiol. Endocrinol. Metab.*, **283**, E217–E225.

Nagamatsu,S., Nakamichi,Y., Yamamura,C., Matsushima,S., Watanabe,T., Ozawa,S., Furukawa,H. and Ishida,H. (1999) Decreased expression of t-SNARE, syntaxin 1, and SNAP-25 in pancreatic β-cells is involved in impaired insulin secretion from diabetic GK rat islets: restoration of decreased t-SNARE proteins improves impaired insulin secretion. *Diabetes*, **48**, 2367–2373.

Namkung,Y. *et al*. (2001) Requirement for the L-type $Ca^{2+}$ channel $\alpha 1_D$ subunit in postnatal pancreatic β cell generation. *J. Clin. Invest.*, **108**, 1015–1022.

Neher,E. (1998) Vesicle pools and $Ca^{2+}$ microdomains: new tools for understanding their roles in neurotransmitter release. *Neuron*, **20**, 389–399.

Norman,R.A. *et al*. (1998) Autosomal genomic scan for loci linked to obesity and energy metabolism in Pima Indians *Am. J. Hum. Genet.*, **62**, 659–668.

Olofsson,C.S., Göpel,S.O., Barg,S., Galvanovskis,J., Ma,X., Salehi,A., Rorsman,P. and Eliasson,L. (2002) Fast insulin secretion reflects exocytosis of docked granules in mouse pancreatic B-cells. *Pflugers Arch.*, **444**, 43–51.

Parker,A. *et al*. (2001) A gene conferring susceptibility to type 2 diabetes in conjunction with obesity is located on chromosome 18p11. *Diabetes*, **50**, 675–680.

Pereverzev,A., Vajna,R., Pfitzer,G., Hescheler,J., Klockner,U. and Schneider,T. (2002) Reduction of insulin secretion in the insulinoma cell line INS-1 by overexpression of a $Ca_v2.3$ ($\alpha 1_E$) calcium channel antisense cassette. *Eur. J. Endocrinol.* **146**, 881–889.

Postic,C. *et al*. (1999) Dual roles for glucokinase in glucose homeostasis as determined by liver and pancreatic β cell-specific gene knockouts using Cre recombinase. *J. Biol. Chem.*, **274**, 305–315.

Pratley,R.E. *et al*. (1998) An autosomal genomic scan for loci linked to prediabetic phenotypes in Pima Indians. *J. Clin. Invest.*, **101**, 1757–1764.

Reetz,A., Solimena,M., Matteoli,M., Folli,F., Takei,K. and De Camilli,P. (1991) GABA and pancreatic β cells: colocalization of glutamic acid decarboxylase (GAD) and GABA with synaptic-like microvesicles suggests their role in GABA storage and secretion. *EMBO J.*, **10**, 1275–1284.

Regazzi,R. *et al*. (1995) VAMP-2 and cellubrevin are expressed in pancreatic β-cells and are essential for $Ca^{2+}$- but not for GTPγS-induced insulin secretion. *EMBO J.*, **14**, 2723–2730.

Renström,E., Eliasson,L., Bokvist,K. and Rorsman,P. (1996) Cooling inhibits exocytosis in single mouse pancreatic B-cells by suppression of granule mobilization. *J. Physiol.*, **494**, 41–52.

Ribalet,B. and Beigelman,P.M. (1981) Effects of divalent cations on β-cell electrical activity. *Am. J. Physiol.*, **241**, 59–67.

Rosario,L.M., Barbosa,R.M., Antunes,C.M., Silva,A.M., Abrunhosa,C.M. and Santos,R.M. (1993) Bursting electrical activity in pancreatic β-cells: evidence that the channel underlying the burst is sensitive to $Ca^{2+}$ influx through L-type $Ca^{2+}$ channels. *Pflugers Arch.*, **424**, 439–447.

Salehi,A., Chen,D., Håkansson,R., Nordin,G. and Lundquist,I. (1999) Gastrectomy induces impaired insulin and glucagon secretion: evidence for a gastro-insular axis in mice. *J. Physiol.*, **514**, 579–593.

Seisenberger,C. *et al*. (2000) Functional embryonic cardiomyocytes after disruption of the L-type $\alpha_{1C}$ ($Ca_v1.2$) calcium channel gene in the mouse. *J. Biol. Chem.*, **275**, 39193–3999.

Takahashi,N., Kadowaki,T., Yazaki,Y., Miyashita,Y. and Kasai,H. (1997) Multiple exocytotic pathways in pancreatic β cells. *J. Cell Biol.*, **138**, 55–64.

Tsunoda,K., Sanke,T., Nakagawa,T., Furuta,H. and Nanjo,K. (2001) Single nucleotide polymorphism (D68D, T to C) in the syntaxin 1A gene correlates to age at onset and insulin requirement in Type II diabetic patients. *Diabetologia*, **44**, 2092–2097.

UKPDS16 (United Kingdom Prospective Diabetes Study Group) (1995) Overview of 6 years therapy of type II diabetes: a progressive disease (UKPDS16). *Diabetes*, **44**, 1249–1258.

Vajna,R. *et al*. (2001) Functional coupling between 'R-type' $Ca^{2+}$ channels and insulin secretion in the insulinoma cell line INS-1. *Eur. J. Biochem.*, **268**, 1066–1075.

Wang,W., Xu,J. and Kirsch,T. (2002) Annexin-mediated $Ca^{2+}$ influx regulates growth plate chondrocyte maturation and apoptosis. *J. Biol. Chem.*, in press.

Wiser,O., Trus,M., Hernandez,A., Renström,E., Barg,S., Rorsman,P. and Atlas,D. (1999) The voltage sensitive Lc-type $Ca^{2+}$ channel is functionally coupled to the exocytotic machinery. *Proc. Natl Acad. Sci. USA*., **96**, 248–253.

Yang,S.N. *et al*. (1999) Syntaxin 1 interacts with the L(D) subtype of voltage-gated $Ca^{2+}$ channels in pancreatic β cells. *Proc. Natl Acad. Sci. USA*, **96**, 10164–10169.

Zhang,W., Khan,A., Östenson,C-G., Berggren,P-O., Efendic,S. and Meister,B. (2002) Down-regulated expression of exocytotic proteins in pancreatic islets of diabetic GK rats. *Biochem. Biophys. Res. Commun.*, **291**, 1038–1044.

*Received February 2, 2003; revised May 15, 2003; accepted June 16, 2003*